Boosting the efficiency of aqueous solar cells: A photoelectrochemical estimation on the effectiveness of TiCl4 treatment

Boosting the efficiency of aqueous solar cells: a photoelectrochemical estimation on the effectiveness of $TiCl_4$ treatment

Federico **Bella**,[1,*] Simone **Galliano**,[2] Giulia **Piana**,[1] Giulia **Giacona**,[1,2] Guido **Viscardi**,[2] Michael **Grätzel**,[3] Claudia **Barolo**[2,4,*], Claudio **Gerbaldi**[1,*]

1) GAME Lab, Department of Applied Science and Technology - DISAT, Politecnico di Torino, Corso Duca degli Abruzzi 24, 10129 – Torino, Italy
2) Department of Chemistry, NIS Interdepartmental Centre and INSTM Reference Centre, Università degli Studi di Torino, Via Pietro Giuria 7, 10125 - Torino, Italy
3) Laboratory of Photonics and Interfaces, Institut des Sciences et Ingénierie Chimiques, Ecole Polytechnique Fédérale de Lausanne (EPFL), Station 3, CH1015 – Lausanne, Switzerland
4) ICxT Interdepartmental Centre, Università degli Studi di Torino, Lungo Dora Siena 100, 10153 – Torino, Italy

Corresponding authors: Federico Bella (federico.bella@polito.it, +39 0110904643), Claudia Barolo (claudia.barolo@unito.it, +39 0116707594) and Claudio Gerbaldi (claudio.gerbaldi@polito.it, +39 0110904643).

Abstract: Increasing the photocurrent is one of the main objectives of the current research on aqueous photovoltaic cells, the emerging green, alternative technology in solar energy conversion devices. In such a scenario, this work deals with the thorough understanding of the electrochemical and photoelectrochemical effects of the $TiCl_4$ treatment onto TiO_2 electrodes, a well-known process for traditional dye-sensitized solar cells, and here, to our knowledge, investigated for the first time in water-based systems. From the quantitative evaluation of the photoelectrochemical parameters, it emerges that the $TiCl_4$ treatment beneficially affects the photovoltaic parameters: it doubles the sunlight conversion efficiency values, inhibits the recombination of photogenerated electrons with oxidized redox mediator ions, and ensures stable and reproducible cell performance at the laboratory scale.

Keywords: Dye-sensitized solar cell; Aqueous electrolyte; $TiCl_4$ treatment; Recombination; Photocurrent.

1. Introduction

Aqueous electrolytes represent the new frontier of dye-sensitized solar cells (DSSCs), as they guarantee sustainability, safety and durability at the same time [1,2]. After the initial concerns on the possibility of replacing nitrile-based organic solvents by water in the

electrolyte, today the number of publications focused on the development of aqueous DSSCs with reasonably good efficiency values is rapidly increasing [3,4,5]. Noteworthy, these solar cells have recently been integrated with redox flow batteries, which demonstrate their ability to photocharge energy storage devices [6]. Efficiency values close to 6% have already been reported for 100% water-based DSSCs [7] and the current research is focused on the investigation of all the different cell components, including novel sensitizers [5,8], unconventional redox pairs [9,10], stable cathodes [11,12], surface treatments of the photoanode [13,14] and of the redox mediator [15,16].

Treatments of the photoelectrode that leads to the creation of an extra nanolayer of TiO_2 (before and/or after the deposition of the standard layer) are well exploited methods to improve the performance of standard DSSCs [17,18,19]. Post-treatment process can be carried out by $TiCl_3$ electrodeposition or titanium isopropoxide post-treatment, but the use of titanium tetrachloride ($TiCl_4$) represents the most successful choice, which leads to the highest increase in the solar cell efficiency [20,21]. Annealing at 450 °C converts species from the $TiCl_4$ solution to TiO_2 crystallites onto the TiO_2 nanocrystalline film surface. This results in improved DSSC performance due to the increased active surface area of the electrode films, enhanced dye loading, inhibited charge recombination by barrier effect and, correspondingly, increased light harvesting efficiency. On one hand, the $TiCl_4$ treatment produces a downward shift in the quasi fermi level (even if other authors proposed an increase of the density of electronic traps corresponding to defective TiO_2 surface sites [20,22]); nonetheless, on the other hand, it does not affect greatly the DSSC potential because it induces a strong reduction of the recombination rate.

In such a scenario, the quantification and proper understanding of the effectiveness of the $TiCl_4$ treatment on the performance of aqueous DSSCs assembled with TiO_2

photoelectrodes have never been studied, especially in combination with an organic dye. This evaluation is of fundamental importance, also considering the rapid and progressive integration of aqueous DSSCs in hybrid photovoltaic devices. Hence, we propose here a thorough investigation of the procedure (in terms of experimental parameters) for $TiCl_4$ treatment and its effects on the efficiency and long-term stability of laboratory scale assembled cells, thus finally demonstrating why and in which circumstances the $TiCl_4$ treatment is able to greatly increase the performance of these emerging aqueous photovoltaic devices. In the current renaissance of DSSCs [23], the present findings pave the way to a wider knowledge of the quantitative effects of the $TiCl_4$ treatment in different electrolyte environments.

2. Experimental

2.1 Materials

Sodium iodide (NaI), iodine (I_2), titanium tetrachloride ($TiCl_4$), chenodeoxycholic acid (CDCA), chloroplatinic acid (H_2PtCl_6), ethanol, acetone, *tert*-butanol (*t*-BuOH) and acetonitrile (ACN) were purchased from Sigma-Aldrich. Deionized water (DI-H_2O, 18 MΩ cm^{-1} at 25 °C) was obtained by Direct-Q 3 UV Water Purification System (Millipore). Sensitizing dye 2-[{4-[4-(2,2-diphenylethenyl)phenyl]-1,2,3,3a,4,8b-hexahydrocyclopento[b]indole-7-yl}methylidene]-cyanoacetic acid (D131) was purchased from Inabata Europe S.A.; the energy levels of the frontier orbitals are –1.26 and 1.04 V *vs.* NHE for LUMO and HOMO, respectively [24,25]. Fluorine-doped tin oxide (FTO) glass plates (sheet resistance 7 Ω sq^{-1}, purchased from Solaronix) were cut into 2 cm × 1.5 cm sheets and used as substrates for the fabrication of both the photoanodes and the counter electrodes [26,27,28].

2.2 Fabrication of the electrodes

FTO-covered glasses were rinsed in mixed acetone/ethanol in an ultrasonic bath for 10 min; solvent traces were removed by flash evaporation at 450 °C on a hotplate. Front electrodes were prepared by depositing a single layer of porous TiO_2 on top of the conductive substrate by means of a manual screen printer with a 43T mesh frame. After deposition of the paste (18NR-T, Dyesol) and 20 min rest to let it bed thoroughly, the TiO_2 layer was dried at 80 °C for 20 min; finally, it was sintered increasing the temperature up to 480 °C in 45 min. The fabricated photoanodes had a thickness of ≈6 μm and active area of 0.25 cm^2. They were finally reactivated by heating at 450 °C for 20 min and, subsequently, soaked into a D131 dye solution (0.50 mM in *t*-BuOH:ACN 1:1, CDCA was added to the dye solution as coadsorbent as detailed below). Dipping in dye solutions was carried out at 22 °C for 5 h under dark conditions and shaking in a Buchi Syncore platform equipped with a cooling plate [29]. After dye loading, photoanodes were washed in acetone to remove residual dye not specifically adsorbed onto the TiO_2 layer [30,31,32,33,34].

DSSCs fabricated in this work are distinguished in four categories, based on the kind of $TiCl_4$ treatment performed: i) Untreated (namely, $TiCl_4$-free); ii) $TiCl_4$-treated onto the FTO substrate ($TiCl_4$ on FTO); iii) $TiCl_4$-treated onto the TiO_2 substrate ($TiCl_4$ on TiO_2); iv) $TiCl_4$-treated (twice) onto both the TiO_2 and the FTO surfaces ($TiCl_4$ on TiO_2+FTO). When treated, substrates were incubated for 30 min into a 40 mM $TiCl_4$ aqueous solution at 70 °C, then washed in deionized water, dried with nitrogen gas, and heat treated at 450 °C for 30 min [35,36,37,38,39].

As regards the preparation of the counter electrodes, FTO conductive glasses were platinized by spreading a H_2PtCl_6 5.0 mM solution onto the plate surface and heating up to 400 °C by a hot plate.

2.3 Fabrication and characterization of aqueous DSSCs

Photoanodes were faced to the counter electrodes exploiting Surlyn® thermoplastic frames (internal area 0.6 cm × 0.6 cm) as spacers (60 μm thick), taking care of the overlapping of the active areas. These components were assembled by hot pressing (20 s) at 110 °C. The electrolyte solution (consisting of NaI and I_2 dissolved in CDCA saturated water) was injected by vacuum backfilling process through a hole in the Surlyn® frame, which was then sealed by commercial epoxy glue [40].

In a previous work [41], we identified – by means of a chemometric approach – the two best conditions for photoanode sensitization and electrolyte formulation of additive-free truly 100% aqueous DSSCs. Exploiting the previous expertise in this respect, here we developed the two optimised lab-scale DSSCs, namely System 1 and System 2 in **Table 1**, which were used to investigate the $TiCl_4$ treatment effects.

Table 1. Photoanode sensitization conditions and electrolyte formulation of aqueous DSSCs studied in this work.

	CDCA:Dye molar ratio	[NaI] (M)	[I_2] (mM)
System 1	18:1	5.0	10
System 2	50:1	1.0	10

Photovoltaic performances were evaluated recording three consecutive photocurrent density *vs.* photovoltage curves on a Keithley 2420 Source Measure Unit, keeping a scan rate equal to 20 mV s^{-1}. Cells were irradiated under simulated 1 sun light intensity (100

mW cm^{-2}, AM 1.5G) after calibration by silicon diode. Electrochemical impedance spectroscopy (EIS) data were obtained by a CH Instruments Inc. Model 680 potentiostat in the frequency range between 100 kHz and 0.1 Hz. The amplitude of the AC signal was 10 mV. Spectra were recorded under dark conditions at applied DC potentials equal to the previously measured V_{oc} values under 1 sun [42,43,44,45,46]. Open circuit voltage decay (OCVD) measurements were performed using the above mentioned potentiostat; DSSCs were kept under constant illumination at the open-circuit conditions, and then the illumination was interrupted and the voltage decay recorded as a function of time.

3. Results and Discussion

3.1 $TiCl_4$ treatment: effect on photovoltaic parameters

The experimental study on the effects of $TiCl_4$ treatment was carried out on two different types of cells, namely System 1 and System 2, having the higher and lower dye coverage and redox mediator contents, respectively, which were deeply characterised in a previous work [41]. These two cells provided similar PCE values (1.25 and 0.95%, respectively), which were nonetheless obtained by rather different characteristic parameters (see **Table 2**). Indeed, the cell fabricated following System 1 showed higher J_{sc} and lower V_{oc} with respect to its counterpart (System 2), as expected for a DSSC containing high amount of sensitizer molecules on the photoanode and iodine species in the electrolyte. UV-Vis spectra of thin photoanodes are given in **Figure A.1** in **Appendix A**.

The $TiCl_4$ treatment was performed for 30 min onto the FTO substrate, onto the TiO_2 film or on both these layers (in the latter case, the process was repeated twice). Photocurrent density *vs.* photovoltage curves of the resulting aqueous DSSCs are shown in **Figure 1**, and the corresponding photovoltaic parameters [i.e., short-circuit current

density (J_{sc}), open-circuit potential (V_{oc}), fill factor (FF) and power conversion efficiency (PCE)] are listed in **Table 2**.

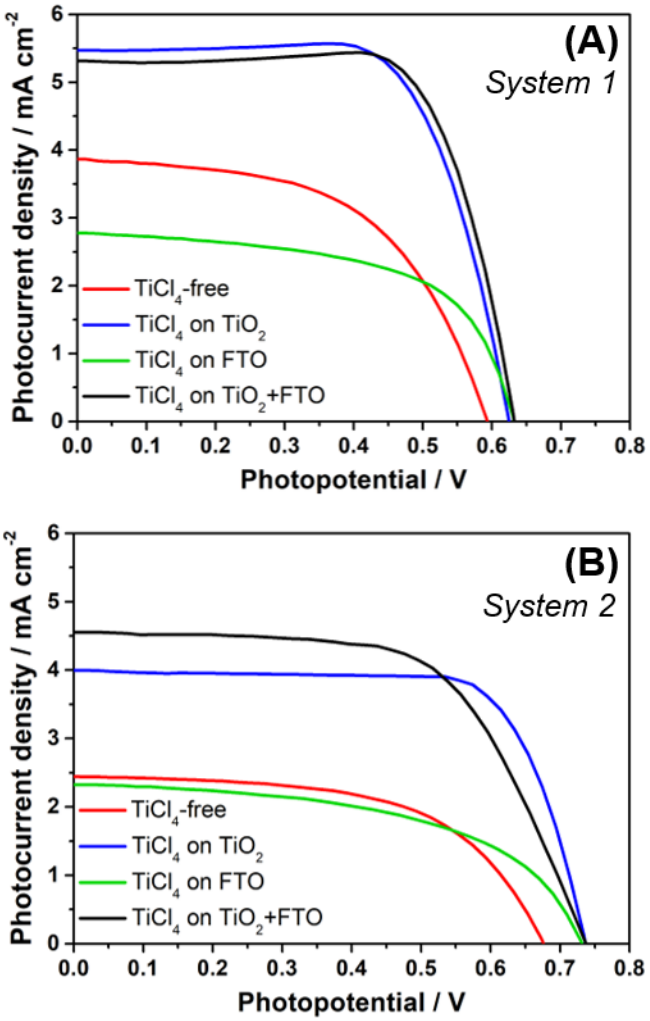

Figure 1. Photocurrent density *vs.* photovoltage curves (measured under 1 sun irradiation) for aqueous DSSCs with different $TiCl_4$ treatments. Cells were fabricated accordingly to the protocols developed for System 1 (A) and System 2 (B).

Table 2. Photovoltaic parameters of aqueous DSSCs fabricated following different $TiCl_4$ treatments. The last column describes the efficiency variation with respect to the pristine ($TiCl_4$-free) device. Reported values are the best values of a batch of 3 cells; the average of the photovoltaic values is given in brackets.

	Cell	J_{sc} (mA cm^{-2})	V_{oc} (V)	FF	PCE (%)	ΔPCE
System 1	$TiCl_4$-free	3.86 [3.81	0.59 [0.58	0.55 [0.54	1.25 [1.19	–

		±0.05]	±0.01]	±0.01]	±0.08]	
	$TiCl_4$ on TiO_2	5.46 [5.40 ±0.08]	0.62 [0.61 ±0.02]	0.70 [0.70 ±0.01]	2.37 [2.31 ±0.10]	+90%
	$TiCl_4$ on FTO	2.77 [2.73 ±0.04]	0.63 [0.62 ±0.01]	0.59 [0.58 ±0.02]	1.03 [0.98 ±0.06]	–18%
	$TiCl_4$ on TiO_2+FTO	5.31 [5.26 ±0.10]	0.63 [0.62 ±0.02]	0.73 [0.72 ±0.02]	2.43 [2.35 ±0.10]	+94%
System 2	$TiCl_4$-free	2.44 [2.41 ±0.04]	0.67 [0.67 ±0.01]	0.58 [0.58 ±0.01]	0.95 [0.94 ±0.05]	–
	$TiCl_4$ on TiO_2	4.10 [4.05 ±0.06]	0.73 [0.72 ±0.01]	0.74 [0.73 ±0.02]	2.17 [2.13 ±0.07]	+128%
	$TiCl_4$ on FTO	2.33 [2.31 ±0.03]	0.73 [0.72 ±0.02]	0.53 [0.53 ±0.01]	0.91 [0.88 ±0.05]	–4%
	$TiCl_4$ on TiO_2+FTO	4.56 [4.53 ±0.05]	0.74 [0.73 ±0.02]	0.62 [0.61 ±0.03]	2.10 [2.02 ±0.09]	+121%

The treatment carried out only onto the FTO substrate led to a decreased J_{sc} and increased V_{oc}, which overall accounted for reduced PCE values by 4 and 18% for System 1 and System 2, respectively. This $TiCl_4$ treatment caused the formation of a nanolayer of TiO_2 onto the FTO substrate, which behaved as a classical blocking layer thus hindering, at least partially, the recombination between the electrons and the oxidized redox couple [47,48]. However, we noticed that this treatment also lowered the J_{sc} values (–28% in the case of System 1, -4% in the case of System 2). To completely understand this effect further experiments are required, which fall out the scope of this paper. Following the literature in the field it is possible to attribute this behaviour to a moderate blocking of the electron flow between the photoanode and the FTO substrate or to a worsening of the interface between the FTO and the mesoporous TiO_2 caused by the additional layer [49].

In a second attempt, the $TiCl_4$ treatment was carried out only onto the TiO_2 film previously deposited by screen-printing and, subsequently, sintered. Photocurrent density *vs.* photovoltage curves shown in **Figure 1** markedly highlight the performance improvements with respect to the untreated cells. All of the three photovoltaic parameters (i.e., J_{sc}, V_{oc} and FF) remarkably increased, leading to PCE values boosted by 90 and 128% (with respect to the pristine samples) for the cells fabricated accordingly to both System 1 and System 2, respectively. Such a result clearly shows that, regardless of the sensitization conditions or the electrolytes formulation, the $TiCl_4$ treatment onto the TiO_2 electrode is fundamental to enhance the performance of aqueous DSSCs. Nevertheless, the quantitative effect is not equal in the two systems, reflecting their different photovoltaic parameters. In fact, in the presence of $TiCl_4$ post treatment, System 1 remains higher in efficiency, but the difference respect to System 2 was substantially reduced (+31% in pristine cells, +12% in post treated cells).

The downward shift in the quasi-Fermi level and the reduction of the recombination rate described in the seminal researches by O'Regan and coworkers [20,21] are both clearly reflected in the J_{sc} and V_{oc} variations in this work with respect to untreated photoanodes. J_{sc} values registered the most significant increase, likely ascribed to higher electron injection efficiency as a consequence of the enlarged energy gap between the semiconductor conduction band and excited dye.

Based on the downward shift in the quasi-Fermi level mentioned in the previous paragraph, we would have expected lower V_{oc} values, which was not the case in the previous work. On the contrary, we observed a relatively small enhancement of the V_{oc} (within the experimental error) that could be ascribed to both a reduction of the

recombination phenomena at the TiO_2/electrolyte interface and to the presence of CDCA in the sensitization solution.

Even if a thorough experimental/theoretical investigation of the quasi-Fermi level downward shift (in the vacuum scale) is out of the scope of this work, for the sake of the readers it is necessary to highlight that, after the initial seminal studies by Sommeling and O'Regan [20,21], several studies and hypothesis have been proposed in the literature. For example, it is well known that the $TiCl_4$ treatment produces the rutile allotrope of TiO_2, regardless of annealing temperature, and consisting of rod-shaped particles [50]. Therefore, a rutile/anatase interface is present on $TiCl_4$-treated photoanodes. Even if some recent experiments led to a possible attribution of the downshift of conduction band maximum to rutile [51], the true fundamentals behind this interface are far from being clearly understood.

3.2 $TiCl_4$ treatment: EIS and OCVD analyses

To shed light on the phenomena described above, EIS and OCVD analyses were performed on the aqueous DSSCs. The Nyquist plots of the impedance response of $TiCl_4$-treated (on TiO_2) and untreated cells of System 2, measured under dark conditions at the V_{oc}, are shown in **Figure 2A**, while the EIS parameters obtained fitting the experimental points (with the equivalent circuit shown in the inset of **Figure 2A**) are listed in **Table 3**. The first semicircle is related to the charge transfer at the TiO_2/electrolyte interface, while the second one (at lower frequencies) corresponds to the diffusion of the redox mediator in the electrolyte. Considering that the diameter of the high frequency semicircle indicates the recombination resistance at the photoanode/electrolyte interface (R_{ct}), **Figure 2A** shows that the $TiCl_4$ treatment performed onto the TiO_2-based photoanode partially

inhibited the recombination processes occurring between I_3^- ions and injected electrons. This is consistent with the higher V_{oc} values measured for $TiCl_4$-treated cells and shown in **Table 2**. As a consequence, such reduction in the recombination rate allowed the flux of injected electrons to build up a higher density of charge in the TiO_2 electrode and this effect compensated for the downward shift of the band edge [20]. The above reported EIS spectra were obtained by the polarization of the photoanode at V_{oc} in dark condition. It is worth to mention that such an approach allows to investigate the electrochemical (rather than photoelectrochemical) properties of the different electrode.

Nyquist plots show that the response due to the processes at the counter-electrode/electrolyte interface are convoluted in the central main semicircle. This is typically observed for aqueous DSSCs [8,13,41,52]. A hypothesis related to the presence of only two semicircles could be based on strongly reduced recombination phenomena in aqueous DSSCs, leading to a wide central semicircle superimposed to the one typically observed at high frequency and related to the Pt/electrolyte interface. This is rather close to what proposed in 1998 by Lindquist's group, who wrote that water molecules, being strongly adsorbed onto the TiO_2 surface, coordinated with the surface Ti atoms and blocked the reaction of I_3^- with the electrons in the TiO_2 conduction band; as a result, V_{oc} increased proportionally to the amount of water introduced in the cell [53].

In order to investigate the $TiCl_4$ effect on photopotential values, OCVD experiments were carried out. **Figure 2B** shows that the cells were initially kept under constant illumination and open-circuit conditions, and then the illumination was interrupted and the voltage decay was recorded as a function of time. During this time, the previously photogenerated electrons underwent recombination, thus reducing their population to a dark equilibrium state. In the resulting curve, higher slopes (measured just after light was

switched off) indicate faster recombination phenomena. The untreated DSSC showed a higher slope with respect to the $TiCl_4$-treated counterpart; the fitted experimental points in the very initial moments after light switching-off gave a 38% enhanced recombination rate for the untreated cell.

The OCVD experiment is also an indirect method for measuring the lifetime (τ_n) of injected electrons, accordingly to the equation:

$$\tau_n = -\frac{k_B \cdot T}{e} \cdot \left(\frac{dV_{oc}}{dt}\right)^{-1} \qquad \text{Eq. 1}$$

where k_B is the Boltzmann constant, T is temperature, and e is the electron charge [54]. The equation provided τ_n values equal to 279 and 201 ms for treated and untreated DSSCs, respectively, thus confirming the increased lifetime for electrons photoinjected into a $TiCl_4$-treated photoanode.

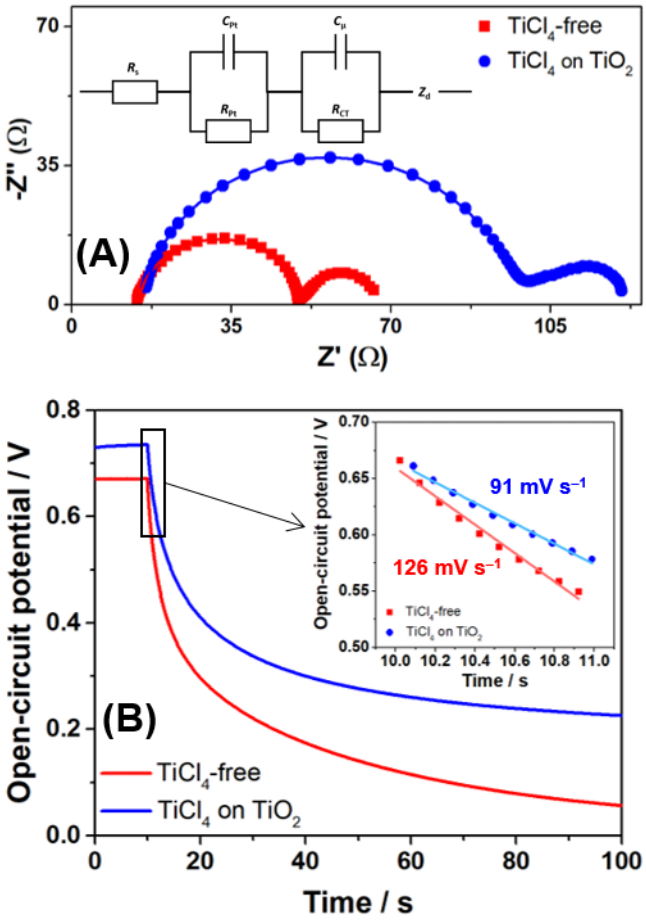

Figure 2. **A)** Nyquist plots and **B)** OCVD curves for aqueous DSSCs with and without $TiCl_4$ treatment. Cells were fabricated accordingly to the protocol developed for System 2.

Table 3. Fitted EIS parameters for aqueous DSSCs with and without $TiCl_4$ treatment. Cells were fabricated accordingly to the protocol developed for system 2.

Cell	R_s (Ω)	R_{ct} (Ω)	C_μ (F)	Z_d (Ω)
$TiCl_4$-free	14.7	35.8	1.06×10^{-6}	17.9
$TiCl_4$ on TiO_2	15.7	82.5	5.12×10^{-6}	23.3

As a further experiment, the $TiCl_4$ treatment was carried out twice, firstly onto the FTO substrate and then onto the TiO_2 film. Based on the analysis of the photovoltaic parameters listed in **Table 2**, we may exclude a synergistic effect on the PCE values, which resulted indeed very similar to the one obtained for $TiCl_4$ on TiO_2 only. Therefore, double $TiCl_4$ treatment does not enhance the PV parameters so markedly to justify its

exploitation, particularly from the practical application viewpoint. As a result, in the followings we will just consider $TiCl_4$ treatment carried out onto the TiO_2 electrode only.

In this work, we also studied the effect of the time of $TiCl_4$ treatment on aqueous DSSC performances. From the analysis of the experiments carried out in our laboratory, we may confirm that the treatment time (i.e., the duration of electrodes immersion in the $TiCl_4$ solution) had a relevant effect on the photovoltaic parameters of the resulting aqueous DSSCs. In particular, by increasing the treatment time from 30 to 90 min, an improvement in the current was measured (from 4.19 to 4.60 mA cm^{-2}), in parallel to a faint decrease in potential values (from 0.71 to 0.70 V), the latter being less significant because within the experimental error. Overall, these variations positively affected the PCE values, which increased from 2.01 to 2.29%, corresponding to a +14% improvement. As an example, photocurrent density *vs.* photovoltage curves for aqueous DSSCs with $TiCl_4$-treated TiO_2 electrodes for 30 and 90 min are shown in **Figure 3**.

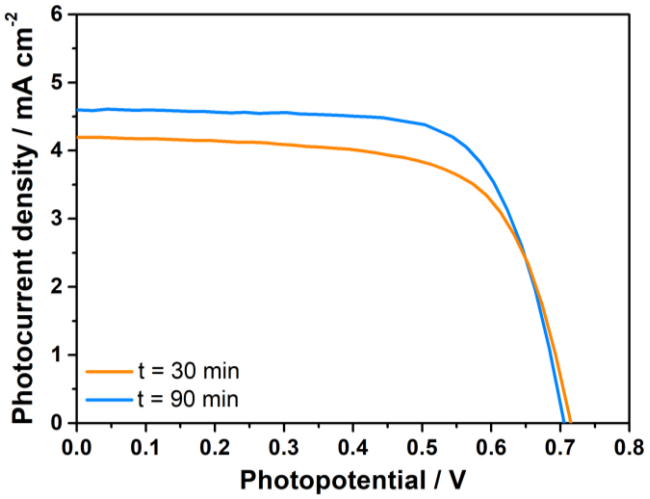

Figure 3. Photocurrent density *vs.* photovoltage curves (measured under 1 sun irradiation) for aqueous DSSCs assembled with TiO_2 electrodes, which were subjected to different $TiCl_4$-treatment (i.e., 30 and 90 min of immersion time in the $TiCl_4$ solution). Cells were fabricated by the following protocol: CDCA:Dye molar ratio = 50:1, [NaI] = 5.0 M, [I_2] = 10 mM.

3.3 $TiCl_4$ treatment: stability issues

The performances of aqueous DSSCs fabricated with $TiCl_4$-treated electrodes were measured for 16 days (≈400 h), keeping the cells at ambient temperature under standard indoor light. In details, cells were placed on a laboratory bench exposing the photoanode side towards the ceiling, where standard low pressure white-yellow neon lamps for ambient irradiation were switched on 12 h per day. Data for untreated cells were already reported in our previous work and were satisfactory [52].

Figure 4 shows the variation of each photovoltaic parameter for two different batches consisting of four cells each, assembled following the protocols of System 1 and System 2, respectively. Overall, both batches of cells were rather stable, thus accounting for the stable performance of the sustainable device components proposed in this study. The photovoltaic parameters values also showed similar variation trends in the two batches: over time, FF values remained almost constant, J_{sc} slightly decreased and V_{oc} progressively increased. The slight V_{oc} increase in the first days was already observed by other research groups in recent years [55]; it was attributed to a sort of activation of the photoanode after cell assembly. As regards the photocurrent, the cells fabricated accordingly to the protocol of System 2 experienced a more pronounced decrease (–25%) than those of System 1 (–6%). This variation is likely ascribed to the lower amounts of both dye and redox couple contained in the cells assembled following System 2. As a result, little variations that may occur over time (e.g., leakage of electrolyte, degradation of some components upon prolonged cell working, etc.) may significantly impact on the proper operation of the device; on the contrary, in the other batch (System 1) the excess quantity of both dye and redox couple justified the negligible effect on the photocurrent values.

Overall, after 16 days, cells assembled following the protocol of System 2 showed a limited 15% decrease of PCE with respect to the initial value, and cells assembled following the protocol of System 1 underwent a remarkable 8% increase. This is encouraging if we consider that recent literature articles showed lower stability trends for aqueous DSSCs, with more marked decreases compared to our present results: –25% in 200 h (1 sun, [11]), –20% in 2 h (dark, [56]), –37% in 4 h (1 sun, [57]), –50% in 2 h (dark, [58]). The cells we present here, characterized by a light yellow colour and a transparent substrate, would be suitable for indoor applications.

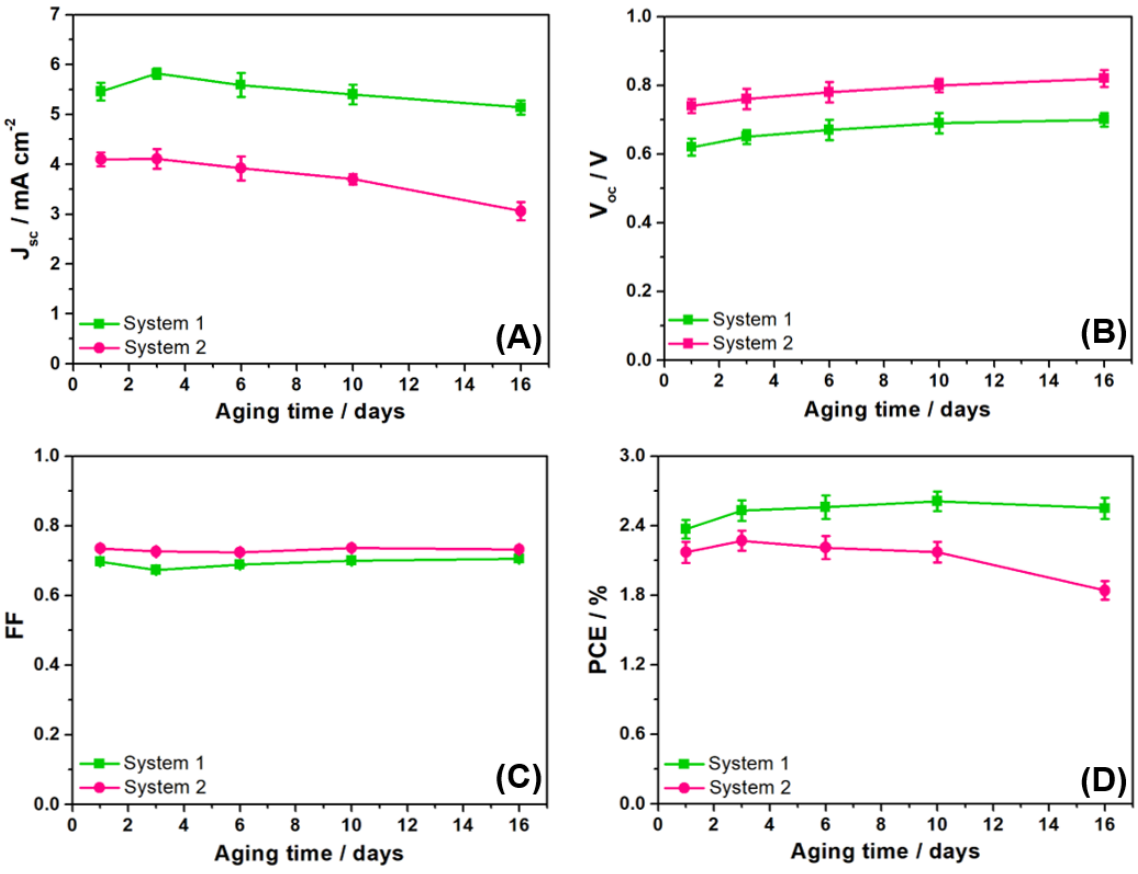

Figure 4. Photovoltaic parameters *vs.* storage time for aqueous DSSCs kept at ambient temperature under natural indoor light. Each data represents the average of a batch of 4 devices fabricated following the protocols of System 1 and System 2 for the $TiCl_4$-treated (on TiO_2) cells.

4. Conclusions

This work demonstrated from a quantitative viewpoint the electrochemical and photoelectrochemical effects of the $TiCl_4$ treatment carried out on TiO_2 electrodes for aqueous solar cells. Regardless of the sensitization process of the photoanode and the composition of the aqueous electrolyte, the sunlight conversion efficiency increased by over 120% when compared to the untreated solar cell counterparts. The electrochemical and photoelectrochemical investigation showed that both the photocurrent and the potential increased as a result of the $TiCl_4$ treatment, and the decrease of the recombination phenomena at the electrode/electrolyte interface is evidenced by an increase of about 40% of the lifetime of photogenerated electrons.

It is worth noting that 100% water-based solar cells can be reproducibly fabricated with efficiencies close to 2.5%, without any additive in the electrolyte nor redox pairs based on heavy metals like cobalt. This work represents a solid benchmark for future studies on these truly sustainable novel photoelectrochemical cells, which are under intense investigation from the scientific community worldwide.

References

[1] F. Bella, C. Gerbaldi, C. Barolo, M. Grätzel, Aqueous dye-sensitized solar cells, Chem. Soc. Rev. 44 (2015) 3431.

[2] C.T. Li, R.Y.Y. Lin, J.T. Lin, Sensitizers for aqueous-based solar cells, Chem. Asian J. 12 (2017) 486.

[3] R. Cisneros, M. Beley, F. Lapicque, P.C. Gros, Hydrophilic ethylene-glycol-based ruthenium sensitizers for aqueous dye-sensitized solar cells, Eur. J. Inorg. Chem. 2016 (2016) 33.

[4] W. Xiang, J. Marlow, P. Bäuerle, U. Bach, L. Spiccia, Aqueous p-type dye-sensitized solar cells based on a tris(1,2-diaminoethane)cobalt(II)/(III) redox mediator, Green Chem. 18 (2016) 6659.

[5] R. Fayad, T.A. Shoker, T.H. Ghaddar, High photo-currents with a zwitterionic thiocyanate-free dye in aqueous-based dye sensitized solar cells, Dalton Trans. 45 (2016) 5622.

[6] W.D. McCulloch, M. Yu, Y. Wu, pH-tuning a solar redox flow battery for integrated energy conversion and storage, ACS Energy Lett. 1 (2016) 578.

[7] R.Y.Y. Lin, F.L. Wu, C.T. Li, P.Y. Chen, K.C. Ho, J.T. Lin, High-performance aqueous/organic dye-sensitized solar cells based on sensitizers containing triethylene oxide methyl ether, ChemSusChem 8 (2015) 2503.

[8] H. Choi, B.S. Jeong, K. Do, M.J. Ju, K. Song, J. Ko, Aqueous electrolyte based dye-sensitized solar cells using organic sensitizers, New J. Chem. 37 (2013) 329.

[9] R.Y.Y. Lin, T.M. Chuang, F.L. Wu, P.Y. Chen, T.C. Chu, J.S. Ni, M.S. Fan, Y.H. Lo, K.C. Ho, J.T. Lin, Anthracene/phenothiazine π-conjugated sensitizers for dye-sensitized solar cells using redox mediator in organic and water-based solvents, ChemSusChem 8 (2015) 105.

[10] W. Yang, M. Söderberg, A.I.K. Eriksson, G. Boschloo, Efficient aqueous dye-sensitized solar cell electrolytes based on a TEMPO/$TEMPO^+$ redox couple, RSC Adv. 5 (2015) 26706.

[11] H. Ellis, R. Jiang, S. Ye, A. Hagfeldt, G. Boschloo, Development of high efficiency 100% aqueous cobalt electrolyte dye-sensitised solar cells, Phys. Chem. Chem. Phys. 18 (2016) 8419.

[12] R. Kato, F. Kato, K. Oyaizu, H. Nishide, Redox-active hydroxy-TEMPO radical immobilized in Nafion layer for an aqueous electrolyte-based and dye-sensitized solar cell, Chem. Lett. 43 (2014) 480.

[13] C. Dong, W. Xiang, F. Huang, D. Fu, W. Huang, U. Bach, Y.B. Cheng, X. Li, L. Spiccia, Controlling interfacial recombination in aqueous dye-sensitized solar cells by octadecyltrichlorosilane surface treatment, Angew. Chem. Int. Ed. 53 (2014) 6933.

[14] H.T. Son, C. Prasittichai, J.E. Mondloch, L. Luo, J. Wu, D.W. Kim, O.K. Farha, J.T. Hupp, Dye stabilization and enhanced photoelectrode wettability in water-based dye-sensitized solar cells through post-assembly atomic layer deposition of TiO_2, J. Am. Chem. Soc. 135 (2013) 11529.

[15] W. Xiang, D. Chen, R.A. Caruso, Y.B. Cheng, U. Bach, L. Spiccia, The effect of the scattering layer in dye-sensitized solar cells employing a cobalt-based aqueous gel electrolyte, ChemSusChem 8 (2015) 3704.

[16] F. Bella, S. Galliano, M. Falco, G. Viscardi, C. Barolo, M. Grätzel, C. Gerbaldi, Approaching truly sustainable solar cells by the use of water and cellulose derivatives, Green Chem. 19 (2017) 1043.

[17 S.W. Lee, K.S. Ahn, K. Zhu, N.R. Neale, A.J. Frank, Effects of $TiCl_4$ treatment of nanoporous TiO_2 films on morphology, light harvesting, and charge-carrier dynamics in dye-sensitized solar cells, J. Phys. Chem. C 116 (2012) 21285.

[18] H. Choi, C. Nahm, J. Kim, J. Moon, S. Nam, D.R. Jung, B. Park, The effect of $TiCl_4$-treated TiO_2 compact layer on the performance of dye-sensitized solar cell, Curr. Appl Phys. 12 (2012) 737.

[19] A. Burke, S. Ito, H. Snaith, U. Bach, J. Kwiatkowski, M. Grätzel, The function of a TiO_2 compact layer in dye-sensitized solar cells incorporating "planar" organic dyes, Nano Lett. 8 (2008) 977.

[20] P.M. Sommeling, B.C. O'Regan, R.R. Haswell, H.J.P. Smit, N.J. Bakker, J.J.T. Smits, J.M. Kroon, J.A.M. Van Roosmalen, Influence of a $TiCl_4$ post-treatment on nanocrystalline TiO_2 films in dye-sensitized solar cells, J. Phys. Chem. B 110 (2006) 19191.

[21] B.C. O'Regan, J.R. Durrant, P.M. Sommeling, N.J. Bakker, Influence of the $TiCl_4$ treatment on nanocrystalline TiO_2 films in dye-sensitized solar cells. 2. Charge density, band edge shifts, and quantification of recombination losses at short circuit, J. Phys. Chem. C 111 (2007) 14001.

[22] M. Jankulovska, T. Berger, S.S. Wong, R. Gómez, T. Lana-Villarreal, Trap states in TiO_2 films made of nanowires, nanotubes or nanoparticles: an electrochemical study, ChemPhysChem 13 (2012) 3008.

[23] L. Kavan, Electrochemistry and dye-sensitized solar cells, Curr. Opin. Electrochem. 2 (2017) 88.

[24] T. Le Bahers, T. Pauporté, G. Scalmani, C. Adamo, I. Ciofini, A TD-DFT investigation of ground and excited state properties in indoline dyes used for dye-sensitized solar cells, Phys. Chem. Chem. Phys. 11 (2009) 11276.

[25] K. Kakiage, Y. Aoyama, T. Yano, K. Oya, J.I. Fujisawa, M. Hanaya, Chem. Commun. 51 (2015) 15894.

[26] J.P. Bantang, D. Camacho, Gelling polysaccharide as the electrolyte matrix in a dye-sensitized solar cell, Materiali in Tehnologije 51 (2017) 823.

[27] X. Wang, P. Li, X.X. Han, Y. Kitahama, B. Zhao, Y. Ozaki, An enhanced degree of charge transfer in dye-sensitized solar cells with a ZnO-TiO_2/N3/Ag structure as revealed by surface-enhanced Raman scattering, Nanoscale 9 (2017) 15303.

[28] S.H. Li, C.R. Zhang, L.H. Yuan, M.L. Zhang, Y.H. Chen, Z.J. Liu, H.S. Chen, The role of electronic donor moieties in porphyrin dye sensitizers for solar cells: electronic structures and excitation related properties, J. Renewable Sustainable Energy 9 (2017) art. no. 053505.

[29] S. Galliano, F. Bella, C. Gerbaldi, M. Falco, G. Viscardi, M. Grätzel, C. Barolo, Photoanode/electrolyte interface stability in aqueous dye-sensitized solar cells, Energy Tech. 5 (2017) 300.

[30] J. Huang, N. Yao, X. Deng, K. Fu, S. Chen, Enhanced efficiency of dye-sensitized solar cells benefited from graphene modified by Ag nanoparticles, J. Nanosci. Nanotechnol. 18 (2018) 3693.

[31] T.M.W.J. Bandara, A.M.J.S. Weerasinghe, M.A.K.L. Dissanayake, G.K.R. Senadeera, M. Furlani, I. Albinsson, B.E. Mellander, Characterization of poly (vinylidene fluoride-co-hexafluoropropylene) (PVdF-HFP) nanofiber membrane based quasi solid electrolytes and their application in a dye sensitized solar cell, Electrochim. Acta 266 (2018) 276.

[32] M.M. Szindler, M. Szindler, L.A. Dobrzanski, The structure and conductivity of polyelectrolyte based on MEH-PPV and potassium iodide (KI) for dye-sensitized solar cells, Open Physics 15 (2017) 1022.

[33] G. Syrrokostas, A. Antonelou, G. Leftheriotis, S.N. Yannopoulos, Electrochemical properties and long-term stability of molybdenum disulfide and platinum counter electrodes for solar cells: a comparative study, Electrochim. Acta 267 (2018) 110.

[34] S. Venkatesan, E.S. Darlim, I.P. Liu, Y.L. Lee, Performance enhancement effects of dispersed graphene oxide sponge nanofillers on the liquid electrolytes of dye-sensitized solar cells, Carbon 132 (2018) 71.

[35] I. Sagaidak, G. Huertas, A. Nguyen Van Nhien, F. Sauvage, New iodide-based amino acid molecules for more sustainable electrolytes in dye-sensitized solar cells, Green Chem. 20 (2018) 1059.

[36] F. Behrouznejad, N. Taghavinia, N. Ghazyani, Monolithic dye sensitized solar cell with metal foil counter electrode, Org. Electron. 57 (2018) 194.

[37] S. Wanwong, W. Sangkhun, J. Wootthikanokkhan, The effect of co-sensitization methods between N719 and boron dipyrromethene triads on dye-sensitized solar cell performance, RSC Adv. 8 (2018) 9202.

[38] S. Alwin, V. Ramasubbu, X. Sahaya Shajan, TiO_2 aerogel–metal organic framework nanocomposite: a new class of photoanode material for dye-sensitized solar cell applications, Bull. Mater. Sci. 41 (2018) art. no. 27.

[39] K.P.S. Zanoni, R.C. Amaral, N.Y. Murakami Iha, F.D. Abreu, I.M.M. de Carvalho, Versatile ruthenium(II) dye towards blue-light emitter and dye-sensitizer for solar cells, Spectrochim. Acta, Part A 198 (2018) 331.

[40] R. Tagliaferro, D. Gentilini, S. Mastroianni, A. Zampetti, A. Gagliardi, T.M. Brown, A. Reale, A. Di Carlo, Integrated tandem dye solar cells, RSC Adv. 3 (2013) 20273.

[41] S. Galliano, F. Bella, G. Piana, G. Giacona, G. Viscardi, C. Gerbaldi, M. Grätzel, C. Barolo, Finely tuning electrolytes and photoanodes in aqueous solar cells by experimental design, Sol. Energy 163 (2018) 251.

[42] Y.C. Chen, Y.J. Li, Y.K. Hsu, Enhanced performance of ZnO-based dye-sensitized solar cells by glucose treatment, J. Alloys Compd. 748 (2018) 382.

[43] S.M. Al-Barody, Characterization and thermal study of Schiff-base monomers and its transition metal polychelates and their photovoltaic performance on dye sensitized solar cells, J. Struct. Chem. 59 (2018) 53.

[44] H. Yuan, W. Wang, D. Xu, Q. Xu, J. Xie, X. Chen, T. Zhang, C. Xiong, Y. He, Y. Zhang, Y. Liu, H. Shen, Outdoor testing and ageing of dye-sensitized solar cells for building integrated photovoltaics, Sol. Energy 165 (2018) 233.

[45] L. Yang, Y. Ji, F. Liao, Y. Cheng, Y. Sun, Y. Li, M. Shao, Pt nanoparticle/Si nanowire composites as an excellent catalytic counter electrode for dye-sensitized solar cells, Electrochim. Acta 271 (2018) 261.

[46] M. Bonomo, G. Naponiello, D. Dini, Oxidative dissolution of NiO in aqueous electrolyte: an impedance study, J. Electroanal. Chem. 816 (2018) 205.

[47] A. Elzarka, N. Liu, I. Hwang, M. Kamal, P. Schmuki, Large-diameter TiO_2 nanotubes enable wall engineering with conformal hierarchical decoration and blocking layers for enhanced efficiency in dye-sensitized solar cells (DSSC), Chem. Eur. J. 23 (2017) 12995.

[48] R. Raja, M. Govindaraj, M.D. Antony, K. Krishnan, E. Velusamy, A. Sambandam, M. Subbaiah, V.W. Rayar, Effect of TiO_2/reduced graphene oxide composite thin film as a blocking layer on the efficiency of dye-sensitized solar cells, J. Solid State Electrochem. 21 (2017) 891.

[49] K.I. Jang, E. Hong, J.H. Kim, Effect of an electrodeposited TiO_2 blocking layer on efficiency improvement of dye-sensitized solar cell, Korean J. Chem. Eng. 29 (2012) 356.

[50] N.G. Park, G. Schlichthörl, J. Van De Lagemaat, H.M. Cheong, A. Mascarenhas, A.J. Frank, Dye-sensitized TiO_2 solar cells: structural and photoelectrochemical characterization of nanocrystalline electrodes formed from the hydrolysis of $TiCl_4$, J. Phys. Chem. B 103 (1999) 3308.

[51] P. Deák, J. Kullgren, B. Aradi, T. Frauenheim, L. Kavan, Water splitting and the band edge positions of TiO_2, Electrochim. Acta 199 (2016) 27.

[52] F. Bella, S. Galliano, M. Falco, G. Viscardi, C. Barolo, M. Grätzel, C. Gerbaldi, Unveiling iodine-based electrolytes chemistry in aqueous dye-sensitized solar cells, Chem. Sci. 7 (2016) 4880.

[53] Y. Liu, A. Hagfeldt, X.R. Xiao, S.E. Lindquist, Investigation of influence of redox species on the interfacial energetics of a dye-sensitized nanoporous TiO_2 solar cell, Sol. Energy Mater. Sol. Cells 55 (1998) 267.

[54] J. Bisquert, F. Fabregat-Santiago, I. Mora-Seró, G. Garcia-Belmonte, S. Giménez, Electron lifetime in dye-sensitized solar cells: theory and interpretation of measurements, J. Phys. Chem. C 113 (2009) 17278.

[55] V. Leandri, H. Ellis, E. Gabrielsson, L. Sun, G. Boschloo, A. Hagfeldt, Organic hydrophilic dye for water-based dye-sensitized solar cells, Phys. Chem. Chem. Phys. 16 (2014) 19964.

[56] S. Zhang, G.Y. Dong, B. Lin, J. Qu, N.Y. Yuan, J.N. Ding, Z. Gu, Performance enhancement of aqueous dye-sensitized solar cells via introduction of a quasi-solid-state electrolyte with an inverse opal structure, Sol. Energy 127 (2016) 19.

[57] H. Tian, E. Gabrielsson, P.W. Lohse, N. Vlachopoulos, L. Kloo, A. Hagfeldt, L. Sun, Development of an organic redox couple and organic dyes for aqueous dye-sensitized solar cells, Energy Environ. Sci. 5 (2012) 9752.

[58] T. Daeneke, Y. Uemura, N.W. Duffy, A.J. Mozer, N. Koumura, U. Bach, L. Spiccia, Aqueous dye-sensitized solar cell electrolytes based on the ferricyanide-ferrocyanide redox couple, Adv. Mater. 24 (2012) 1222.